An introduction of Three-Dimensional Precipitation Particles Imager (3D-PPI)

Response to the referees

Jiayi Shi, Xichuan Liu, Lei Liu, Liying Liu, Peng Wang

Response to Anonymous Referee #1

Original Referee comments are in italic

manuscript text is indented, with added text underlined and ~~removed text crossed out.~~

Our responses are in regular font.

Thank you very much for your thorough review and insightful comments on our manuscript. We appreciate the time and effort you have dedicated to evaluating our work and your constructive feedback. Your suggestions have been invaluable in helping us improve the quality and clarity of our manuscript. Below, you will find our point-by-point responses to your comments, along with the revisions made to the manuscript.

Regarding the PSD Calculation Concern:

Equation 8: First off, I'm not an expert on the theory behind PSD calculations. That said, from what I understand, I think the image edge correction needs based on the PSD bin centers rather than for individual particles. Using the bin center in the edge correction would essentially be accounting for the potential volume in which a particle from that size bin could be observed rather than accounting for this volume difference only when a particle is observed. So the sample volume for a PSD bin centered on Di would be

$$V_i = (a - 2D_i) \cdot (b - 2D_i) \cdot d$$

where v, a, b, and d are deffned as per Equation 8 of the manuscript. The depth might also vary with particle size (I know it does with PIP), but exactly how this might vary with particle size is beyond my knowledge.

Thank you for your valuable advice about the calculation of Vi, particularly regarding the image edge correction. We have revised Eq. (8) in the manuscript to incorporate the bin center for the edge correction, as you suggested. Because of the previous addition of equations, Eq. 7 and 8 in the original manuscript correspond to Eq. 9 and 10 in the revised manuscript, as follows:

The time-averaged PSD calculated from 3D-PPI counting over a specified period is as follows:

$$PSD(D_i) = \frac{N_i}{\frac{N_{ima}}{\triangle D_i \cdot \sum_{j=1} V_j}} \quad \mathrm{PSD}(D_i) = \frac{N_i}{\triangle D_i \cdot N_{\mathrm{ima}} \cdot V_i} \qquad \text{(7) (9)}$$

Where N_i is the number of particles in the i^{th} size bin; N_{ima} is the number of acquired images over a period of time; The size descriptor D for 3D-PPI is $D_{\max}$ or D_{eq} in this paper; ~~V_j~~V_i (m^3) is the valid OV of the Cam0 ~~at the j^{th} moment.~~after edge correction. Since we discard particles at the edges of the image in Sec. 4.1, ~~V_j~~V_i is a function of ~~the average particle size at the j^{th} moment~~D_i, shown in Eq. (10~~8~~). The a, b, and d represent the length (0.17m), width (0.125m), and depth (0.~~1043m~~0.088m) of the field of view respectively.

~~$V_j =$~~

$$\begin{cases} \left(a - \overline{D_j}\right) \times b \times d & \text{, when the particles at left or right edges discarded;} \\ a \times \left(b - \overline{D_j}\right) \times d & \text{, when the particles at top or bottom edges discarded;} \\ \left(a - \overline{D_j}\right) \times \left(b - \overline{D_j}\right) \times d & \text{, both conditions exists at the same time;} \\ a \times b \times d & \text{, no edge particles are discarded.} \end{cases}$$

~~(8)~~

$$V_i = (a - 2D_i) \cdot (b - 2D_i) \cdot d \qquad (10)$$

Response to Anonymous Referee #2

Original Referee comments are in italic

manuscript text is indented, with added text underlined and ~~removed text crossed out.~~

Our responses are in regular font.

Thank you very much for your thorough review and insightful comments on our manuscript. We appreciate the time and effort you have dedicated to evaluating our work and your constructive feedback. Your suggestions have been invaluable in helping us improve the quality and clarity of our manuscript. Below, you will find our point-by-point responses to your comments, along with the revisions made to the manuscript.

Observation volume OV and effective OV

The effective OV is the intersection of the three individual OVs, which are 170mmx 125mm x 104mm. The intersection of the two OVs of Cam1 and Cam2 is a cuboid with the dimensions 104mm x 104mm x 125mm, i.e. it has the volume of 1352cm3. Intersecting this with the OV of Cam0 will result in the effective OV, which then must have a smaller volume. That means the volume that you provide with 1464cm3 is wrong. Alternatively, your description is wrong and the effective OV is not the intersection oif the individual OVs.

Thank you for your comments. We apologize for our mistakes. Upon retesting, we found that the depth of field should indeed be 88mm, rather than 104mm, and the effective OV volume should indeed be 775 cm^3, rather than 1464 cm^3. We have promptly corrected this in the revised manuscript.

Rephrase: "the observation volume (OV) ... is the interior rectangle of the observation volume of ..." - 'Interior rectangle' is wrong term to describe a volume - It is not clear to use 'observation volume' to describe 'observation volume'

Thank you for your comments. The"interior rectangle" is indeed a misnomer. We have removed these misrepresentations.

Rephrase: "The cylindrical observation volume of the three telecentric lenses and LED lighting beams of 3D-PPI is illustrated in Fig. 2." - Does this refer to effective OV? - Fig 2 does not show any observation volume (shows beams) - No observation volume is cylindrical

It doesn't refer to effective OV. Fig. 2 shows is the beams of cylindrical lens rather than effective OV.

We have revised this part to make it clearer in the revised manuscript Line 105 and 110:

~~The cylindrical observation volume of the~~The three telecentric lenses and LED lighting beams of 3D-PPI is illustrated in Fig. 2. To clarify, the three dimensions of observation volume (OV) of one high-resolution camera is ~~the interior rectangle of the observation volume of one telecentric lens with three dimensions~~ a × b × d (170mm × 125mm × ~~104mm~~88mm), which represent the length, width, and depth of field of view respectively.

Figure 2. The ~~observation volume~~two views of ~~the~~ three telecentric lenses and LED ~~lighting~~light beams.

Optical resolution / resolving power / smallest resolved detail

Thank you for adopting a better terminology. Pixel resolution and resolution (number of pixels of sensor) of the different cameras are important parameters in describing your instrument. I am missing another paramter describing the optical performance of your cameras, that is the resolving power achieved on images of Cam0-2 and on images of Cam3. You could determine it by calibration or by identifying the smallest features that can be detected on your images. I do not agree with a statement that the "smallest recognizable detail … is 0.0416 mm" (in response to my point 9). Of course, this is theoretically the best limit, however, it is not backed up by evidence. Can you show images of snow particles with small details to illustrate the smallest features that can be detected (under optimal illumination and in-focus position)? You seem to focus on "larger particles" (response to my point 9), but you don't mention this clearly in the manuscript.

Thank you for your comments. We apologize that 'smallest recognizable detail can be detected' was an inaccurate description in the previous reply. Actually, given that the 3D-PPI uses telecentric lenses, it is approximated that all particles within the depth of field (88mm) are well illuminated and clearly imaged. In our manuscipt, we don't take into account the concepts of optical resolution, resolving power and smallest resolved detailed that you mentioned (we know they have different meanings from pixel resolution). The 0.0416 mm just refers to the pixel resoltion indeed the theoretical limit based on the camera's specifications. i.e. a single pixel representing the actual length of 0.0416 mm. The following figure illustrate this point.

Thank you for your understanding!

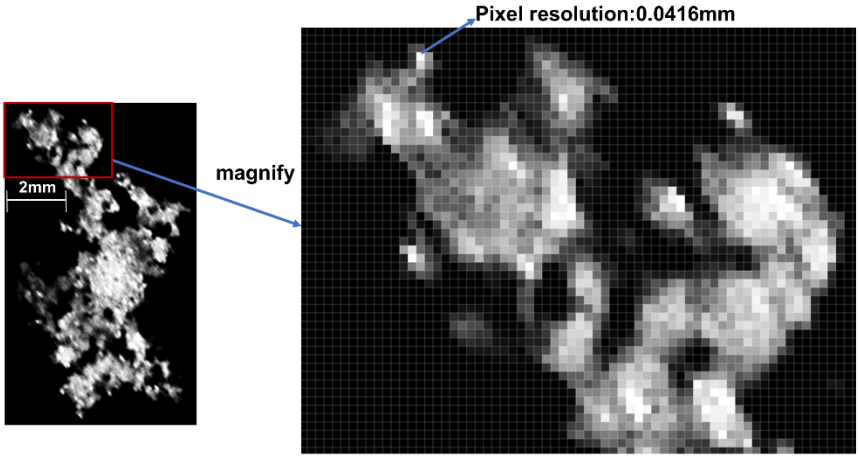

Figure 1. Evidence of pixel resolution

Removal of noise and smaller particles

You are rejecting features with Dmax less than about 0.2mm. I would recommend stating this limit in the Abstract/Conclusions (something like "...measure particles > 0.2 mm").

Thank you for your advice. We have added that our instrument is designed to measure particles with D_{max} greater than 0.2 mm in Conclusion:

> The high-resolution cameras feature a pixel resolution of 41.5 μm·px-1 and are precisely synchronized by clock control which is sufficient to obtain fine shapes of snowflakes larger than 0.2mm, and the large field of view of 170 mm×125 mm enables it to capture enough snowflakes to estimate PSD accurately.

You call it "removal of small noises from image". I would rephrase this as I don't consider 'small noises' a proper term, it sounds colloquial.

Thank you for your advice. We have replaced "small noises " with "pixel noise (no larger than 20 pixels)" to avoid any colloquial implications.

Prior to rejecting small features, you join connected regions that have their centroids separated by less than 4mm. This still fells like a large distance to me. I don't understand why the centroid distance has been chosen here rather than the actual gap separating any two connected regions. The centeroid distnce depends on the size of the connected regions whereas the gap represents the size of a potentially undetected region of the particle. When joining small connected regions you accept a gap of almost 4mm. For larger connected regions, the accepted gap is smaller by roughly the average size of these connected regions. It would be good, after justifying better your joice of criterion, to show examples of particles resulting from joining connected

regions. This could be done in Fig.7 by adding two or three such examples including a length scale for reference. A propoer description of what is shown now in the figure is missing (you indicate (in red numbers) detected particles, I think).

Thank you for your advice. We have also reconsidered our image processing algorithms to joining connected regions. Using centroid distance as a criteria for judgement does bring these problems you mentioned. Instead of using the centroid distance, we have now adopted the distance between the closest points of connected regions as the standard criterion. Given the adoption of the new distance criterion, the minimum threshold for combining should be set at 2 mm rather than 4 mm. The revised Figure 7 now illustrates an example where several closely spaced connected regions are combined into one, and the 2 mm length scale has been added.

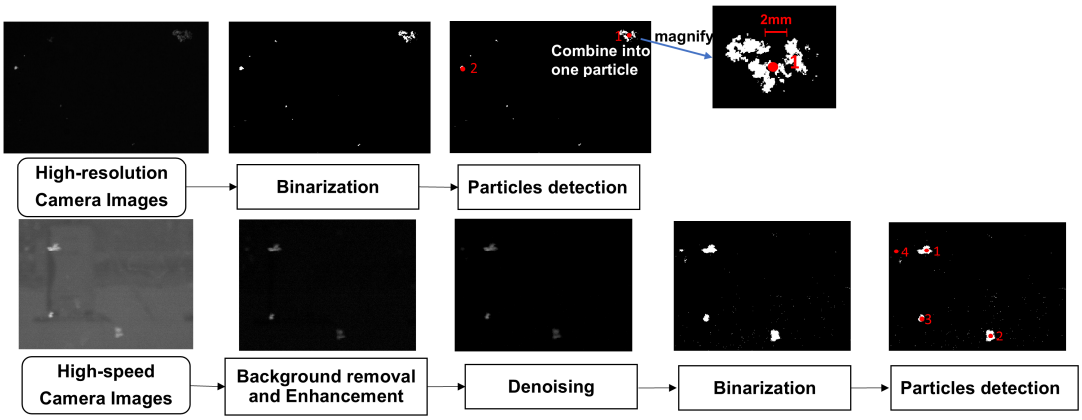

Figure 2. The revised Fig. 8 in the revised manuscipt.

We have revised this part in manuscipt:

> Secondly, combine regions into a single particle when the ~~centroids~~ distance between the closest points of connected regions in a single image ~~are~~ is detected to be less than ~~4~~ 2 mm apart. This step is necessary because a single particle may sometimes be perceived as two separate particles due to its position near the edge of the image processing threshold. Thirdly, discard the particles with an area smaller than 20 pixels (Equivalent to 0.035 mm2, Dmax is about 0.2mm), which enables the removal of ~~small noises~~ pixel noise (no larger than 20 pixels) from the image, to prevent there pixel noises from being mistakenly detected as small snowflakes.

Pixel resolution

You determine the pixel resolution using ceramic spheres of known diameters, as described in Sect 3.2, which you call "Calibration of image binarization". I still find it unclear how you describe the process. You say that "we perform manual adjustments

to mitigate the software's misidentifification" sugesting that you use a software or algorithm. However, you state that the algorithm described in Sect 4 is not used. So, it is unclear what software or algorithm is used here. I think, for the purpose of determining the pixel resolution, it would have been better, and easier to describe, to do a completely manual analysis of the images of the ceramic spheres, for example by adding best-fitting circles and determining their diameters in pixels. I also still believe that taking images of a millimeter scale would have been better for the purpose. Aligning such a millimeter scale would not have been difficult with the required accuracy. Using a millimeter scale would have avoided the dependenc on the used algorithm and/or manual analysis (e.g. different thresholds result in over- or undersizing).

Thank you for your comments. We apologize for our mistakes.

Firstly, As you say we just use ceramic spheres of known diameters to calculate a more accurate pixel resolution for each high-resolution camera. This process is not called "Calibration of image binarization", it is just an essential step before the "Calibration of image binarization". In the revised manuscript, we have placed this process in the added Sec. 3.2: **Estimation of pixel resolution**. And revised Sec. 3.3: **Calibration of image binarization**.

Secondly, actually, we don't use any software or algorithms, as you suggest, we process it entirely manually: taking the approach of counting the number of pixels that the diameter of the sphere occupies in the image.

Thirdly, using millimeter scale indeed a good choice as it comes with its own scale avoiding manual counting. However, the reason for not using the millimeter scale to obtain image resolution are as follows: pixel resolution can only be estimated when the millimeter scale plane is parallel to the camera image plane, which is difficult to guarantee. The advantage of the ceramic sphere in comparison is that its image taken at any angle is round.

*In fact, the use of spheres of know sizes is more suitable for testing an image processing algorithm. You actually do that in Sect 4.1 and Fig. 8. As a consequence, your Figures 6b) and 8 look almost identical, and it is difficult to see what difference there is between the two tests. In one figure you show error bars in the other not. What are the error bars in Fig 8? I guess they are related to that you image 20 spheres falling through in fornt of each camera. For Fig 6b, did you image one sphere for each diameter? Were these spheres dropped as for Fig 8? For Fig.6b, I would suggest to plot the distance of two points (in mm) over the distance of these two points on the image in pixels (rather than the opposite as you are doing). Then you end up with fitting your data to the linear expression of the form Dmax = d*Px + e rather than, as you do now, Px = b*Dmax + c. In these expressions Dmax represents the actual size or distance in mm and Px represents the measured distance on the image in pixels. The fitting coefficients are d and b, respectively, and the intercepts are e and c, respectively. The resulting value for d is the pixel resolution. Whereas you take the inverse of the slope b. It is, however not generally true that d = 1/b, where d and b result from fitting the same data to the above*

*two expressions. So, do the fit of Dmax = d*Px + e to your data in Sect 3.2 and then report d as pixel resolution. You likley get very similar results, but you avoid the confusion of how to comparer or convert your results properly to pixel resolution.*

Fig 6b from one sphere (for each size), or the average of several images of spheres (at each size)?

Thank you for your comments.

Firstly, for Fig. 6b, we used these spheres to estimate the pixel resolution. For Fig. 8b (Fig. 7 of the revised manuscript), we still used these spheres to test the accuracy of the image binarization. These two figures look similar and both use the same spheres, but for different purposes.

Secondly, for Fig. 6b, only one set of measurements was taken for each sphere diameter to fit the slope of the line. In contrast, for Fig. 8b (Fig. 7 of the revised manuscript) shows that each sphere was measured 20 times, with the average of those measurements represented as the center point of the error bars for each diameter. The length of the error bars indicates the uncertainty, expressed as the standard deviation. For Fig 6b, we only image one sphere for each diameter. These spheres indeed dropped as for Fig 8.

Finally, thank you for your advice to switch the horizontal and vertical coordinates of Fig. 6b. We have revised our manuscipt as your suggestions.

Image processing algorithm – resulting errors

You use adaptive thresholding to binarize images. You also state (in the response to my point 14d) that "It has been tested that particles outside the depth of field cannot be clearly imaged and therefore cannot be detected." What does this statement mean? Are particles outside the DOF not properly binarized (because they are fuzzy, not in focus)? My question remains: How well-defined is the depth of field? The PSD values and OVs depend on it. You state that "The average error for all spheres across different diameters is -0.048 mm." In your responses you explain that this error is "measured-true" and can be positive or negative. Taking the average of two errors where one is, for example, +5 and the other -5 would result in a zero average, which would wrongly describe the error. I think this is what happened when you report the very small "average error", it is a misleadingly small value, the average of larger positive and negative values. Consider another way to describe the errors and relative errors.

Thank you for your comments.

Firstly, we have conducted laboratory tests to determine the depth of field (DOF) of our imaging system, shown in Figure 3. We used the Modulation Transfer Function (MTF), which measures the system's ability to resolve contrast at different spatial frequencies. Specifically, we consider the range where the MTF value exceeds 50% of its maximum as the effective depth of field (shown in Figure 4, the DOF is 88mm). As such, any

snowflakes with MTF values below this threshold are deemed fuzzy and considered outside the depth of field. Therefore, our algorithm effectively excludes these particles from identification.

Figure 3. The DOF test scene.

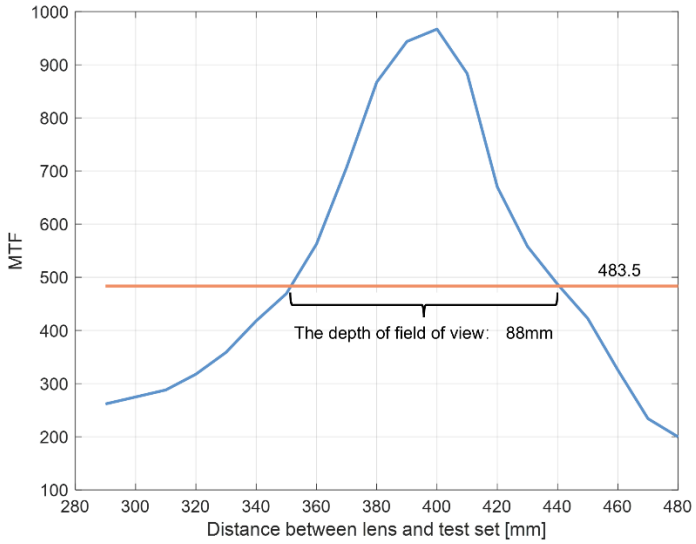

Figure 4. The MTF plot.

Secondly, as you mentioned, averaging the positive and negative errors can lead to misleadingly small values. To provide a clearer and more intuitive presentation of the errors, we have calculated the mean relative error (MSE) for D_{max} and D_{eq} and plotted the relative error bars in Fig. 7 of the revised manuscript, shown in Figure 5

> Regarding the Dmax measurement results (Fig. 7c, e), smaller spheres (9 mm and below) tend to show that the measurements are slightly greater than the true values, while larger particles exhibit that the measurements are slightly lower than the true values. The maximum relative error is about 14%, and the MRE of Dmax is about 4%. As for Deq measurement results (Fig. 7d, f), almost all diameter measurements underestimate the true values. The maximum relative error is about -7% and the

MRE of Deq is about 3%. Since the measurement errors of Deq for all spheres are lower than the true values, they can be utilized for systematic error correction.

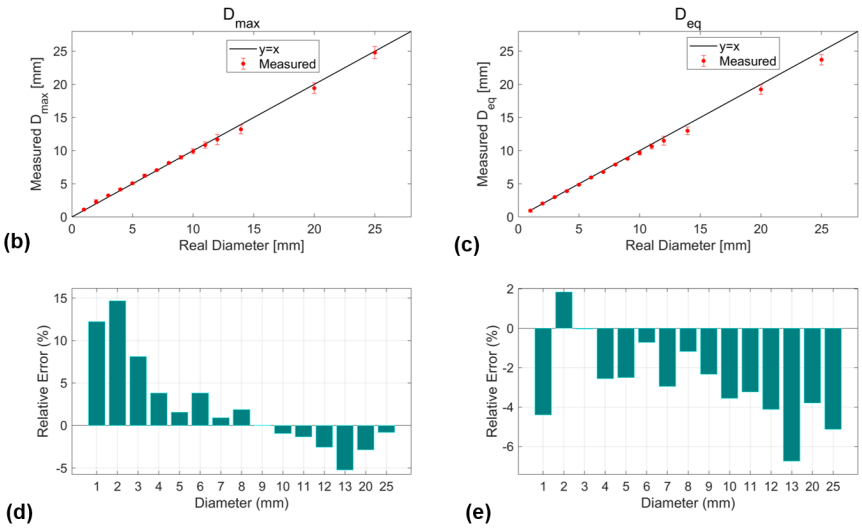

Figure 5. The revised Fig. 7 in the revised manuscipt.

Horizontal speed

"The average value (consider positive and negative) of the horizontal velocity component…" What does that mean? Is this a suitable average (see also error of image processing above).

The statement means that the average horizontal velocity component (+0.41m/s), including both positive and negative values, represents the net directional movement of the particles. In my personal view, this average calculation is appropriate as it provides a direct measure of the overall trend in particle motion, which is essential for our analysis.

It is not obviously clear that the horizontal speed corresponds to the East-West wind direction. Mention that installing the instrument facing south means that the horizontal speed seen by the high-speed camera Cam3 corrsiponds to East-West.

Thank you for your advice, we have mentioned this at the beginning of this paragraph:

> Installing the instrument facing south means that the horizontal velocity seen by the high-speed camera Cam3 corresponds to East-West. The average value ~~(consider positive and negative)~~ of the horizontal velocity component measured by 3D-PPI is +0.41m/s ~~(positive and negative values indicate westward and eastward velocities, respectively)~~, and the standard deviation is 0.73m/s (Fig. 16a). The overall distribution of particle horizontal velocities ranges between ±3m/s, and more than

70% of the snowflakes have a horizontal velocity distribution between ±1m/s. Positive velocities predominate over negative ones, largely influenced by the prevailing westward winds.

Size-dependent OV in Eq. 7

Excluding particles at the edge of the image means a reduction of OV that depends on particle size. You account for that in the modified eq (7). It now features Vj, the valid OV at the "jth moment". Vj has already been used in eq (6) for speed, potentially leading to confusion. However, what confuses me more is this "jth moment", not sure what that means. Should that not be "in the jth image"?

Thank you for your comments. We apologize for our mistakes. V_j here does create confusion with the representation of velocity. And it should be 'in the jth image' rather than 'jth moment'.We have revised Eq. 7 and 8, and all related text, to eliminate the use of " V_j " and "the *j*th moment," which should now prevent any ambiguity in the presentation of our methodology.

Because of the previous addition of equations, Eq. 7 and 8 in the original manuscript correspond to Eq. 9 and 10 in the revised manuscript, as follows:

The time-averaged PSD calculated from 3D-PPI counting over a specified period is as follows:

$$\mathrm{PSD}(D_i) = \frac{N_i}{\triangle D_i \cdot N_{\mathrm{ima}} \cdot V_i} \tag{9}$$

Where N_i is the number of particles in the i^{th} size bin; N_{ima} is the number of acquired images over a period of time; The size descriptor D for 3D-PPI is D_{max} or D_{eq} in this paper; V_i (m^3) is the valid OV of the Cam0 after edge correction. Since we discard particles at the edges of the image in Sec. 4.1, V_i is a function of D_i, shown in Eq. (10). The a, b, and d represent the length (0.17m), width (0.125m), and depth (0.088m) of the field of view respectively.

$$V_i = (a - 2D_i) \cdot (b - 2D_i) \cdot d \tag{10}$$

In the revised manuscript, we have focused on rewriting Sec. 3.2 and 3.3:

3.2 Estimation of pixel resolution

The purpose of this section is to experimentally determine the accurate pixel resolution of each high-resolution camera. The process utilizes 15 spheres with absolute sphericity ranging from 1 to 25 millimeters in diameter, which are dropped into the OV of 3D-PPI (Fig, 6a). The materials of the spheres have a similar refractive index to the snowflakes. Theoretically, any spherical object captured in an image appears as a perfect circle, which is an advantage of using spheres. The ratio of the actual diameter of the sphere (D_a) to its diameter in pixels as represented in the image (D_p) constitutes the pixel resolution. The D_a is measured using a caliper, with units in millimeters, and the D_p is counted manually, with units in pixels. The scatterplot about the D_a and corresponding D_p for 15 ceramic spheres and the linear least-squares fit straight line plotted together (Fig, 6b), resulting in:

$$D_a\,[\mathrm{mm}] = (0.0416 \pm 0.0001) \cdot D_p\,[\mathrm{px}] + 0.0259 \quad (1)$$

for Cam0,

$$D_a\,[\mathrm{mm}] = (0.0410 \pm 0.0003) \cdot D_p\,[\mathrm{px}] + 0.1647 \quad (2)$$

for Cam1, and

$$D_a\,[\mathrm{mm}] = (0.0410 \pm 0.0003) \cdot D_p\,[\mathrm{px}] + 0.0835 \quad (3)$$

for Cam2.

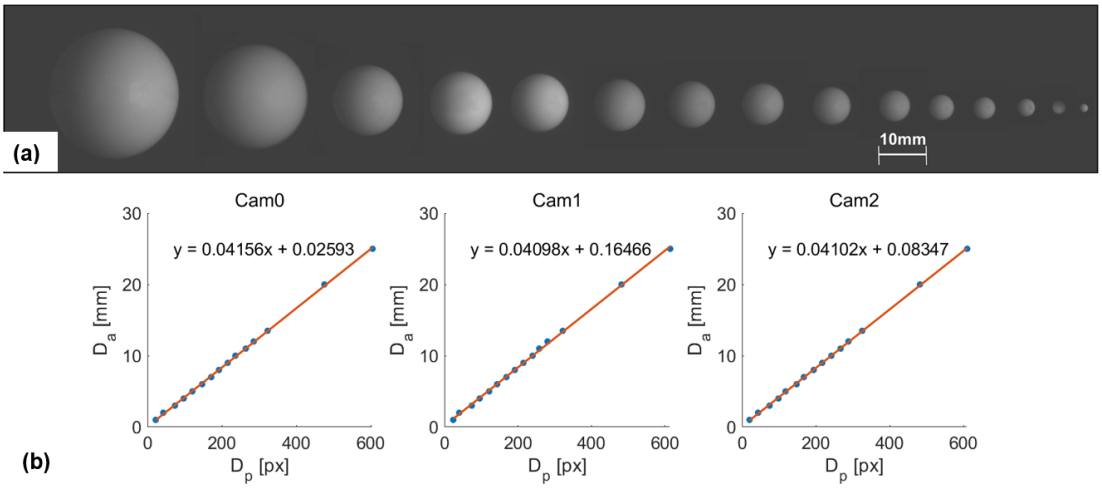

Figure 6. **(a)** The 15 reference spheres ranging from 1 to 25 millimeters in diameter captured by high-resolution; **(b)** The scatterplot about the D_a and corresponding D_p for 15 ceramic spheres and the linear least-squares fit straight line. The results of the linear least squares fit are also shown in the legends.

The reciprocals of the slopes of the three fitted lines are 0.04156, 0.04098, 0.04102 mm·px^{-1}, and closely align with the 0.0416 mm·px^{-1} specification from the manufacturer of the high-resolution cameras. The non-zero intercepts observed in the linear fits, ranging from about 0.02 px to 0.16 px, can be

attributed to several factors, including systematic errors introduced during the calibration process due to lens distortion or misalignment, as well as image processing artifacts from the binarization method that may affect edge detection.

3.3 Calibration of image binarization

The image captured by high-resolution camera is binarized through adaptive thresholding. Adaptive thresholding is a widely used technique for image binarization, where the threshold for converting pixel values to binary is determined based on local characteristics of the image rather than a single global threshold. This method enhances the accuracy of foreground particle detection, particularly in images with complex backgrounds and uneven illumination. The adaptive threshold at a pixel location (u,v) , denoted as $T(u,v)$, represents the threshold value used to classify the pixel at position (u,v) into either foreground or background. It is computed using the local mean $\mu(u,v)$ from a specified neighborhood around that pixel, adjusted by a sensitivity coefficient C:

$$T(u,v) = \mu(u,v) - C \tag{6}$$

Where the sensitivity coefficient C, typically constrained between 0 and 1, plays a crucial role in modulating the threshold. A smaller C value treats relatively lower brightness pixels as foreground, while a larger C value causes more pixels to be classified as background. Therefore, a well-determined C can enhance binarization performance by effectively distinguishing between foreground objects and background noise, thereby improving the segmentation results.

Calibration of image binarization is aimed at determining the optimal value of C. Firstly, drop the spheres of each diameter mentioned in Sec. 3.2 times into the observation volume, and acquire 20 clear images for each diameter (similar to Figure 6a). Secondly, use the adaptive thresholding algorithm to convert the sphere image into the binarized image, and then calculate D_{max} and D_{eq} (in image, the D_{max} is the distance between the two farthest points of the particle profile, and the D_{eq} is the diameter of the circle equal to the area of the particle profile. The D_{max} and D_{eq} are equal only when the image of the sphere is perfectly circular). Thirdly, convert D_{max} and D_{eq} from pixels to millimeters through pixel resolution calculated in Sec. 3.2 and calculate the average value of D_{max} and D_{eq} for 20 times for each diameter.

Ultimately, calculate the mean relative error (MRE) for different sensitivity coefficients C using Eq. (7). And the results in Fig.7a shows that a C value of 0.4 resulted in the smallest MRE, indicating that the optimal value for C is 0.4.

$$\mathrm{MRE} = \frac{1}{2}\left(\frac{1}{n}\sum_{i=1}^{n}\left|\frac{D_{\mathrm{a}i} - \overline{D}_{\mathrm{max}i}}{D_{\mathrm{a}i}}\right| + \frac{1}{n}\sum_{i=1}^{n}\left|\frac{D_{\mathrm{a}i} - \overline{D}_{\mathrm{eq}i}}{D_{\mathrm{a}i}}\right|\right) \tag{7}$$

Where n denotes the number of spheres of different diameters, which is 15; D_{ai} denotes the i^{th} diameter of the sphere;

$\overline{D}_{\mathrm{max}i}$ and $\overline{D}_{\mathrm{eq}i}$ denote the average value of D_{max} and D_{eq} for 20 times for i^{th} diameter respectively.

With C set to 0.4, the 15 spheres in Fig. 6a were effectively binarized, as shown in Fig. 7b. Regarding the D_{max} measurement results (Fig. 7c, e), smaller spheres (9 mm and below) tend to show that the measurements are slightly greater than the true values, while larger particles exhibit that the measurements are slightly lower than the true values. The maximum relative error is about 14%, and the MRE of D_{max} is about 4%. As for D_{eq} measurement results (Fig. 7d, f), almost all diameter measurements underestimate the true values. The maximum relative error is about -7% and the MRE of D_{eq} is about 3%. Since the measurement errors of D_{eq} for all spheres are lower than the true values, they can be utilized for systematic error correction.

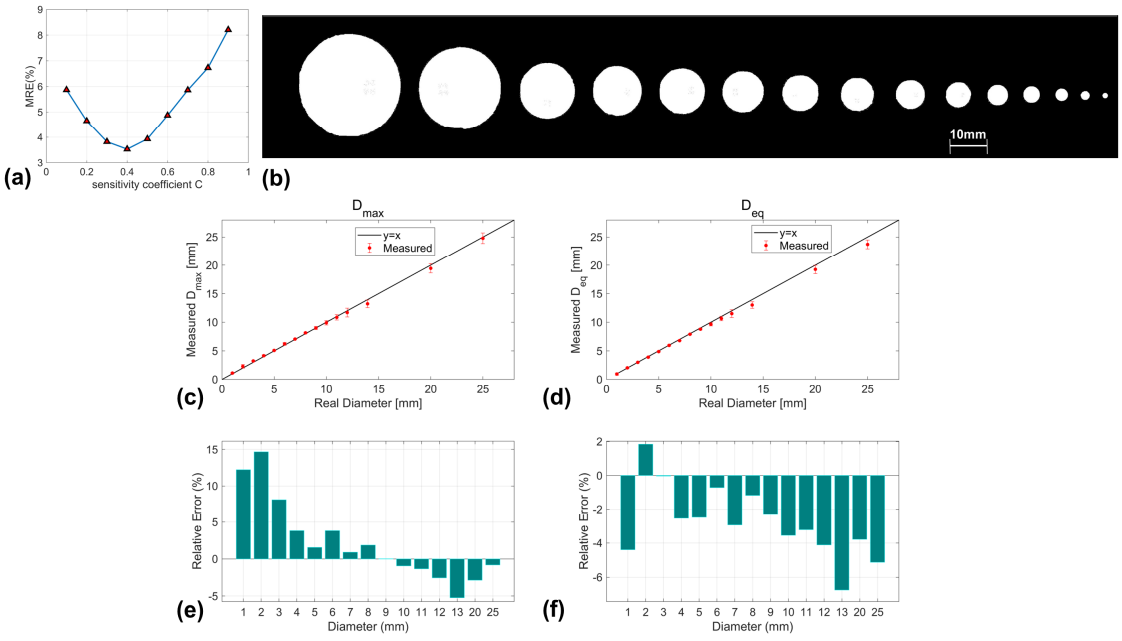

Figure 7 (a) Variation of MRE with sensitivity coefficient C; **(b)** The binarized images of 15 spheres; The average values of measurements of D_{max}**; (c) - (f)** The average values and relative errors of 20 D_{max} and D_{eq} measurements for per diameter sphere.